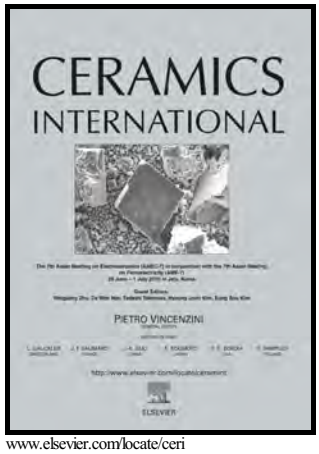

www.elsevier.com/locate/ceri

Crystal structure, microwave dielectric properties and low temperature sintering of $(Al_{0.5}Nb_{0.5})^{4+}$ co-substitution for Ti^{4+} of $LiNb_{0.6}Ti_{0.5}O_3$ ceramics

Enzhu Li, Xin Yang, Hongcheng Yang, Hongyu Yang, Huaibao Sun, Ying Yuan, Shuren Zhang

PII: S0272-8842(18)33361-3
DOI: https://doi.org/10.1016/j.ceramint.2018.11.243
Reference: CERI20217

To appear in: *Ceramics International*

Received date: 11 November 2018
Revised date: 30 November 2018
Accepted date: 30 November 2018

Cite this article as: Enzhu Li, Xin Yang, Hongcheng Yang, Hongyu Yang, Huaibao Sun, Ying Yuan and Shuren Zhang, Crystal structure, microwave dielectric properties and low temperature sintering of $(Al_{0.5}Nb_{0.5})^{4+}$ co-substitution for Ti^{4+} of $LiNb_{0.6}Ti_{0.5}O_3$ ceramics, *Ceramics International,* https://doi.org/10.1016/j.ceramint.2018.11.243

Crystal structure, microwave dielectric properties and low temperature sintering of $(Al_{0.5}Nb_{0.5})^{4+}$ co-substitution for Ti^{4+} of $LiNb_{0.6}Ti_{0.5}O_3$ ceramics

Enzhu Li[1,2*], Xin Yang[1,2], Hongcheng Yang[1,2], Hongyu Yang[1,2], Huaibao Sun[1,2], Ying Yuan[1,2], Shuren Zhang[1,2]

[1]National Engineering Research Center of Electromagnetic Radiation Control Materials, University of Electronic Science and Technology of China, Chengdu, 610054

[2]Key Laboratory of Multi-Spectral Absorbing Materials and Structures of Ministry of Education, University of Electronic Science and Technology of China, Chengdu, 610054

*Tel: 86-28-8320-6695 Email: lienzhu@uestc.edu.cn (Enzhu Li)

Abstract

The phase composition, microstructure, microwave dielectric properties of $(Al_{0.5}Nb_{0.5})^{4+}$ co-substitution for Ti site in $LiNb_{0.6}Ti_{0.5}O_3$ ceramics and the low temperature sintering behaviors of Li_2O-B_2O_3-SiO_2 (LBS) glass were systematically discussed. XRD patterns and EDS analysis result confirmed that single phase of $Li_{1.075}Nb_{0.625}Ti_{0.45}O_3$ solid solution was formed in all component. The increase of dielectric constant (ε_r) is ascribed to the improvement of bulk density. The restricted growth of grain has a negative influence on quality factor ($Q\times f$) value. The τ_f value could be continuously shifted to near zero as the doping content increases. Great microwave dielectric properties were obtained in $LiNb_{0.6}Ti_{(0.5-x)}(Al_{0.5}Nb_{0.5})_xO_3$ ceramics (x = 0.10) when sintered at 1100℃ for 2 h: ε_r = 70.34, $Q\times f$ = 5144 GHz, τ_f = 4.8ppm/℃. The sintering aid, LBS glass, can effectively reduce the temperature and remain satisfied microwave performance. Excellent microwave dielectric properties for x = 0.10 were obtained with 1.0 wt. % glass: ε_r = 70.16, $Q\times f$ = 4153 GHz (at 4

GHz), τ_f = -0.65ppm/℃ when sintered at 925℃ for 2 h.

Keywords: $LiNb_{0.6}Ti_{0.5}O_3$ ceramics, microwave dielectric properties, Li_2O-B_2O_3-SiO_2 (LBS) glass, low temperature sintering.

1 Introduction

Due to the fast growth of the modern telecommunications devices, lead-free high performance microwave dielectric ceramics with an appropriate property were wildly used [1-4]. Three key properties need to be balanced for these ceramics: a large dielectric permittivity (ε_r), high quality factor ($Q \times f$, where f stands for the resonant frequency) and a near zero temperature coefficient of resonant frequency (τ_f). In addition, a low sintering temperature is necessary for Low Temperature Co-fired Ceramic (LTCC) [5-7].

Recently, a series novel Li-based Li_2O-Nb_2O_5-TiO_2 system dielectric material were studied systematically owing to its excellent performance. $Li_{1+x-y}Nb_{1-x-3y}Ti_{x+4y}O_3$ (M phase) solid solutions was firstly reported by Villafuerte-Castrejon in 1987[8]. On the basis of their research, HRTEM and single-crystal X-ray diffraction was utilized by L. Farber[9] to investigate the structure of M phase, and they illustrated that the solid solutions were consisted of n layers of $LiNbO_3$-type slabs, and a layer of a corundum-type structure ($Ti_2O_3^{2+}$) was inserted in the propagating chains of $LiNbO_3$-like chains, and n is dependent on the content of Ti. Albina Y. Borisevich[10] introduced the microwave characterization of M phase. And then, for the purpose of improving the dielectric characterization of M phase, lots of researchers have made many attempts. For instance, the ε_r will increase and τ_f can be adjusted to near zero while a small number of Ca^{2+} substitutes for Ti^{4+}. Due to the inevitable volatilization of Li element during high temperature sintering, excessive Li was used, which enhanced the microwave characterization subsequently[11, 12].

The τ_f value reflects stability of ceramics, and a near zero τ_f value means that the ceramics can work stably in a temperature range[13]. To adjust the τ_f value of $LiNb_{0.6}Ti_{0.5}O_3$ (30.6 ppm/℃), a solid solution was designed, after referring the radius of $(Al_{0.5}Nb_{0.5})^{4+}$ (IR=0.588Å CN=6) and Ti^{4+}(IR=0.605Å CN=6).Besides, Zhang

report that the complex substitution of Al^{3+} and Nb^{5+} for Ti^{4+} gives rise to an phase transition and then adjust the dielectric performance[14].

Furthermore, along with the developments in LTCC technology, ceramics that could be sintered at low sintering temperature become more and more important[15, 16]. However, most modern commercial materials including LNT have a high processing temperature, which is higher than the melting point of high-electrical-conductivity electrode (Ag~961℃,Cu~1042℃)[17]. Hence, a lot of attempts to reduce the sintering temperature had been carried out [18, 19]. For example, V_2O_5, B_2O_3 and Bi_2O_3 was effectively reduce the sintering temperature of M phase and still maintain excellent performance[20-22]. However, boron trioxide is easily soluble in ethanol, water, and the functional hydroxyl group in PVB would react readily with boron. Besides, vanadium pentoxide is difficult to disperse uniformly in the matrix material, and the viscosity of the slurry containing V_2O_5 dielectric material is large. The mentioned problems will make it difficult to obtain a dense cast film strip, and serious quality control problems occur in the manufacture of LTCC[23, 24]. Therefore, suitable sintering aid plays a vital role for the application in LTCC of M phase solid solutions.

Combining with our previous work, LBS glass has large solubility in ZnO-Nb_2O_5-TiO_2 systems[25-27]. Considering the great compatibility with Nb_2O_5-based system, LBS glass was adopted for lowing the temperature sintering. In addition, the effects of LBS on the crystal structure, microstructure, properties and the low temperature mechanism was also discussed.

2 Experimental

High purity Li_2CO_3, Nb_2O_5, TiO_2 and Al_2O_3 were weighted according to the non-stoichiometric ratio of $LiNb_{0.6}Ti_{(0.5-x)}(Al_{0.5}Nb_{0.5})_xO_3$ (hereafter abbreviated LNT , $0.06 \leq x \leq 0.14$). These compounds were mixed and ball-milled for 5 h with zirconia media in deionized water. These mixtures were calcined at 870℃ for 3 h. The LBS glass was also synthesized via reagent-grade starting materials: Li_2CO_3, H_3BO_3, SiO_2 (40.04:53.72:6.24 wt. %). After milled for 2 h with zirconia ball and deionized water

as milling media. Then the glass melted into a platinum crucible at 1200℃ for 2 h. The glass melt was then poured into a copper plate to quench, and vibrated mill for 4 h.

Subsequently, the calcined powders were re-milled for 5 h. Afterwards, 6 wt. % PVA was added to pressed into disks (15 mm in diameter and 8 mm in height) at 20 MPa, and then the samples were sintered at 1100℃ for 2 h. With LBS glass added, the calcined LNT powders and LBS were mixed and milled together for 5 h, the mixtures were dried and added with acrylic acid to form pellets, and the specimen were sintered at 850-950℃ for 2 h.

The bulk density of the sintered samples was calculated by Archimedes method. X-ray diffraction (Philips X'Pert ProMPD, Amsterdam, The Netherlands) was performed to confirm the phase composition and Cu kα radiation is provided from the detector. The microstructure of the sample's surface was examined with a scanning electron microscopy (Inspect F). The shrinkage curve of the ceramics was obtained by thermomechanical analyses (TMA) (Model DIL 420C, Netzsch, Germany), with heating rates were 5, 7.5, 10, 12.5, 15 K/min, respectively. Dielectric properties at microwave frequency was obtained by the Hakki-Coleman dielectric resonator method. The measured result was displayed in a network analyzer (Hp83752A, the United States), with the TE_{011} mode. Temperature coefficient value was calculated based on the following formula:

$$\tau_f = \frac{f_T - f_{T_0}}{f_{T_0} \times (T - T_0)} \qquad (1)$$

Where the f_T and f_{T_0} were the TE_{011} resonant frequency at temperature T and T_0, respectively.

3 Results

The room temperature XRD patterns of LNT samples sintered at 1100℃ for 2 h are plotted in Fig. 1. It can be seen that all patterns can be indexed as $Li_{1.075}Nb_{0.625}Ti_{0.45}O_3$ phase (JCPDS # 54-1017). In the whole range, no secondary phase could be detected within the resolution limit of the apparatus, which means that

$(Al_{0.5}Nb_{0.5})^{4+}$ and Ti^{4+} occupied the same position to form a homogeneous solid solution. And the lattice parameters are shown in Table. 1, c-axis decreases linearly only about 0.10%, while a-axis (b-axis) increases about 0.17%, with the increment of doping content. Thus, the unit cell volume is increased inevitably, and the offset of the XRD peak also confirms this, where a similar phenomenon was reported by Mao[28].

Figure 2 shows the SEM images of LNT ceramics with: (a) x = 0.06, (b) x = 0.08, (c) x = 0.10, (d) x = 0.12, (e) x = 0.14 when sintered at 1100℃ for 2 h, and platelet-shaped homogenous microstructures were revealed for all the ceramics. It can be seen that small number of pores can be detected when x≤0.10, while a compact morphology appears at x = 0.12. It means that as the doping content increases, the microstructure of LNT ceramic specimen becomes densified, which could be confirmed by the bulk density in Fig. 2(f). In addition, as the value of x increases, the average size of the grains gradually decreases, which is facilitated the formation of densified structure.

The EDS and mapping analysis were utilized to further reveal the microscopic information of LNT (x = 0.10), as shown in Fig. 3. Obviously, two kinds of crystal grains namely rod-shaped grains (spot A) and plate-shaped grains (spot B) can be detected in the SEM image of all components shown in Fig. 2. EDS analysis results demonstrated that two type grains have similar elemental proportions, which is consistent with the XRD results. Mapping analysis results shows that all elements except aluminum are distributed in the specimen uniformly. As known to all, the grain boundary energy is the driven force of ceramic sintering, and it can be decreased as a result of the segregation of aluminum at the grain boundaries, which results in a decrease in ion diffusion rate. Several mentioned factors will hinder the movement of the grain boundaries, and thus the growth of crystal grains is suppressed[11], which is consistent with the SEM analysis.

The dielectric characterization as a function of the x value (at 3.8~4.1 GHz) are plotted in Fig 4. Although the polarizability of $(Al_{0.5}Nb_{0.5})^{4+}$ (2.38 Å) is smaller than that of Ti^{4+} (2.93 Å)[29], the ε_r of LNT ceramics increased linearly from 67 to 72 while the doping amount increased from 0.06 to 0.14, owing to the improvement of

densification. The dielectric constant of the pores in the microwave frequency band is about 1, which is much lower than the dielectric constant of the LNT phase, therefore, the existence of pores affects the ε_r seriously[30]. Thus, the ε_r value monotonously increases along with the improvement of bulk density. It is well accepted that the Q value of microwave dielectric ceramics is affected by complex factors including intrinsic loss and extrinsic loss. Intrinsic loss is associated with the absorptions of phonon oscillation, extrinsic loss is related to lattice defect, such as impurity, cavity, substitution, grain boundaries, size and second phases, pores, etc[31-34]. From the SEM image, as the doping amount increases, although the improvement of densification will benefit $Q\times f$, the effect of small grains will generate more grain boundaries, which will lead to a drop of $Q\times f$ value[35].

The τ_f value is a key factor for microwave dielectric ceramics. It determines the temperature stability of dielectric ceramics. As is shown in Fig 4, the τ_f of LNT decreased from 24.2 to -14.8 ppm/℃ with the increment of doping content. This implies that the substitution of $(Al_{0.5}Nb_{0.5})^{4+}$ for Ti^{4+} effectively improves τ_f values. As known, τ_f and the permittivity temperature coefficient τ_ε are presented in Equation 1:

$$\tau_f = -(\alpha_l + \frac{1}{2}\tau_\varepsilon) \qquad (1)$$

where α_l represent the linear thermal expansion coefficient. The influence of α_l on τ_f can be ignored since α_l is always in the range of 10ppm/℃. Therefore, τ_f values is mainly determined by τ_ε, which is deduced by the following formula:

$$\tau_\varepsilon = \frac{1}{\varepsilon}\left(\frac{\partial\varepsilon}{\partial T}\right) = \frac{(\varepsilon-1)(\varepsilon+2)}{3\varepsilon}\times(A+B+C) \qquad (2)$$

$$A = -\frac{1}{V}\left(\frac{\partial V}{\partial T}\right)_P \qquad (3)$$

$$B = \frac{1}{\alpha_D}\left(\frac{\partial \alpha_D}{\partial V}\right)_T \times \left(\frac{\partial V}{\partial T}\right)_P \qquad (4)$$

$$C = \frac{1}{\alpha_D}\left(\frac{\partial \alpha_D}{\partial T}\right)_V \qquad (5)$$

where α_D is the ionic polarizability. According to the theory of Bosman et al.[36], generally, the sum of the A and B terms is approximately 6±1ppm/℃. And C is in the range of -1 to -10 ppm/℃. Since the range of change of C is bigger than the sum of A and B, it is expected that τ_ε will largely depend on C. Lee[37] believes that the C is related to the crystal structure and cell parameters. And according to Yoon et al. [38], the unit cell volume has a strongly positive correlation with the lattice energy, subsequently, τ_ε should be proportional to the cell volume. Corresponding to the lattice parameter shown in Table 1, the unit cell volume increases with the increase of x, so the τ_ε keeps increasing, as a result, the resonant frequency temperature coefficient τ_f decrease as the $(Al_{0.5}Nb_{0.5})^{4+}$ incorporation increases.

The LNT ceramics sintered at 1100℃ shows excellent microwave properties. However, the sintering temperature is not suitable for the requirement in LTCC. Thus, glass frit with a chemical composition of Li_2O-B_2O_3-SiO_2 (LBS) was chosen to lower the sintering temperature of the component with the best temperature stability as x = 0.10, and the amount of LBS was selected as 0.5~2.0 wt. %.

The XRD patterns of LNT ceramics sintered at their optimal temperature with different content of LBS (Fig 5(a)) and different temperature with 1.0 % LBS (Fig 5(b)) are exhibited. All diffraction peaks can be indexed to $Li_{1.075}Nb_{0.625}Ti_{0.45}O_3$ (JCPDS # 54-1017). No second phase appeared, indicating that a single phase of LNT was obtained at low sintering temperature.

The SEM images of the as-fired surfaces of LNT samples sintered at 925°C with different amount of LBS are shown in Fig.6 (a)-(d), the corresponding EDS analysis of 1.0 wt. % LBS was also provided. The EDS results revealed that the bright white area is the LNT grain and the gray area is the glass phase. All samples exhibit a uniform grain size and liquid phase appears. More fused glass was observed as the additive content increases, which is benefit for packing the ceramics to improve the densification. However, when the sintering aid exceeds an appropriate content (1.0 wt. %), the glass phase would deteriorate the performance of the specimen because of the poor performance of LBS (ε_r = 7.58, tanδ(%) = 0.45, τ_f = − 86 ppm/°C)[27].

The variations of ε_r value and bulk density of each composition sintered at

various temperature are plotted in Fig.7. As shown, the curves for different content of glass doped samples are analogous. The density of each samples increases with the increase of sintering temperature and then remains saturated. The densities of the specimens doped with 0.5 wt. % LBS sintered at 850℃ remain relatively low while the LBS glass content increased to above 1.0 wt. %, the samples could reach high densities (4.11g/cm^3) at around 925℃. Besides, XRD results shown that no second phase formed during sintering, and the dielectric polarizability of LNT remains unchanged, the density and the additives should be should be a key factor for the change in ε_r value. The variations of ε_r value represents an analogous trend with the bulk density. Only when the sintering temperature and the number of additives are appropriate, the ε_r can reach the optimum value.

The fluctuation of $Q\times f$ value at different sintering conditions are plotted in Fig 8(a). Generally speaking, the change of $Q\times f$ and bulk density are consistent. The insufficient performance of the ceramics with 0.5wt. % glass sintered at 850 °C arises from the poor densification. After increasing the sintering temperature, the $Q\times f$ value increased sharply. A relatively good performance has been obtained when the content of the glass is 1.0 wt. % because of a high densification, which can be confirmed in Fig 8(a). It is worthy to note that when the glass content is high (≥1.5wt. %), a negative influence on the $Q\times f$ value shows due to the formation of a large amount of liquid phase.

Figure 8(b) shows the τ_f and ε_r of LNT with 1.0 wt. % LBS. Since LBS glass has a negative τ_f values of -86 ppm/℃[27], the τ_f value of the system decrease after the addition of glass. And the τ_f value increases towards to zero with the increase of sintering temperature shows a similar trend to the ε_r. The microwave dielectric properties of typically high ε_r LTCC materials are summarized in Tab 2 [3, 27, 39-43].

For further investigate the sintering mechanism of LNT with LBS, the shrinkage curves of LNT samples added with 1.0 wt. % LBS under a sintering rate between 5-15 K/min are shown in Fig. 9. The samples un-doped glass starts to shrink at about 850℃, and shrinkage reaches to maximum(15.2%) when the temperature reaches 1150℃. After adding a small content of LBS (1.0 wt. %), the samples begin to shrink at 650℃.

For better exploring liquid phase sintering mechanism, the activation energies (E_a) which represents the minimum energy to meet the ceramic densification requirements during sintering of LNT ceramic un-doped and doped LBS were calculated according fowling equation:

$$\ln k = -\frac{Ea}{R}\left(\frac{1}{T}\right) + \ln z$$

where R=8.3145 J/K/mol, k is the heating rate of 5 K/min, 7.5 K/min ,10 K/min, 12.5 K/min, 15 K/min, T represents the Kevin temperature(K), z is a constant value.

In addition, the relationship of 1/T versus 1000lnk plots in Fig 10. The fitted results indicate an average E_a value of 455.91±68.00 kJ/mol for un-doped LBS glass and an average E_a of 295.11±77.45 kJ/mol for LNT doped 1.0 wt. % LBS. The decline of Ea also confirm the presence of low-temperature liquid phase produced by LBS glass directly accelerate the low temperature sintering process.

4 Conclusion:

In this work, the $(Al_{0.5}Nb_{0.5})^{4+}$ ionic co-substitutions for Ti^{4+} of $LiNb_{0.6}Ti_{0.5}O_3$ ($0.06 \leq x \leq 0.14$) ceramics was investigated. The XRD patterns and EDS analysis result indicated a formation of $Li_{1.075}Nb_{0.625}Ti_{0.45}O_3$ solid solution without secondary phases. The SEM photograph shows that as the amount of doping increases, an increasingly densified microstructure appears, which bring in the increase of ε_r value. Besides, the small size of grain inevitably leads to an increase of grain boundaries, which have a negative influence on $Q \times f$ value. The τ_f values could be continuously shifted to near zero. Excellent microwave dielectric properties were obtained in LNT ceramics (x = 0.10) when sintered at 1100℃ for 2 h: ε_r = 70.34, $Q \times f$ = 5144 GHz (at 3.85 GHz), τ_f = 4.8ppm/℃. For explore the practical use of LNT ceramics in LTCC field, the responsibility of LBS glass for lowing the sintering temperature, and the relevance of various LBS content to the sintering behavior, activation energy, phase composition, and microwave dielectric properties were also collected in this work. Indeed, LBS glass can reduce the activation energy required for the reaction sintering process, subsequently reducing the sintering temperature from 1100 °C to 925 °C. Satisfied

balance of microwave dielectric properties for x = 0.10 were obtained with 1.0 wt. % glass at 925℃ for 2 h: ε_r = 70.16, $Q \times f$ = 4153 GHz, τ_f = -0.65 ppm/℃.

Acknowledgement

The authors appreciate the financial supports from the National Natural Science Foundation of China (No. 51872037)

References

[1] Z. Pan, X. Yu, Q. Wang, J. Cao, F. Pan, C. Liang, F. Lu, X. Kuang, C. Su, J. Wang, L. Fang, Stabilization and tunable microwave dielectric properties of the rutile polymorph in α-PbO_2-type $GaTaO_4$-based ceramics, J. Mater. Chem.C, 2 (2014) 4957.

[2] B. Liu, L. Li, X.Q. Liu, X.M. Chen, Structural evolution of $SrLaAl_{1-x}(Zn_{0.5}Ti_{0.5})_xO_4$ ceramics and effects on their microwave dielectric properties, J. Mater. Chem.C, 4 (2016) 4684-4691.

[3] D. Zhou, L. X. Pang, D. W. Wang, C. Li, B. B. Jin, I.M. Reaney, High permittivity and low loss microwave dielectrics suitable for 5G resonators and low temperature co-fired ceramic architecture, J. Mater. Chem. C, 5 (2017) 10094-10098.

[4] W. Liu, R. Zuo, Low temperature fired $Ln_2Zr_3(MoO_4)_9$ (Ln=Sm, Nd) microwave dielectric ceramics, Ceram. Int., 43 (2017) 17229-17232.

[5] I.M. Reaney, D. Iddles, Microwave Dielectric Ceramics for Resonators and Filters in Mobile Phone Networks, J. Am. Ceram. Soc., 89 (2006) 2063-2072.

[6] J. Li, L. Fang, H. Luo, Y. Tang, C. Li, Structure and Microwave dielectric properties of a novel temperature stable low-firing $Ba_2LaV_3O_{11}$ ceramic, J. Eur. Ceram. Soc., 36 (2016) 2143-2148.

[7] H. Li, B. Tang, Y. Li, Z. Qing, S. Zhang, Effects of $Mg_{2.05}SiO_{4.05}$ addition on phase structure and microwave properties of $MgTiO_3$–$CaTiO_3$ ceramic system, Mater. Lett., 145 (2015) 30-33.

[8] M.E. Villafuerte Castrejón, A. Aragón Piña, R. Valenzuela, A.R. West, Compound and solid-solution formation in the system Li_2O-Nb_2O_5-TiO_2, J. Solid State Chem., 71 (1987) 103-108.

[9] L. Farber, I. Levin, A. Borisevich, I.E. Grey, R.S. Roth, P.K. Davies, Structural Study of $Li_{1+x-y}Nb_{1-x-3y}Ti_{x+4y}O_3$ Solid Solutions, J. Solid State Chem., 166 (2002) 81-90.

[10] A.Y. Borisevich, P.K. Davies, Crystalline Structure and Dielectric Properties of $Li_{1+x-y}Nb_{1-x-3y}Ti_{x+4y}O_3$M- Phase Solid Solutions, J. Am. Ceram. Soc., 85 (2004) 573-578.

[11] H. Sun, E. Li, H. Yang, H. Yang, S. Zhang, A novel $LiNb_{0.6}Ti_{0.5}O_3$ microwave dielectric ceramic with Ca substitutions, Mater. Lett., 210 (2018) 275-278.

[12] E. Li, M. Zou, S. Duan, N. Xu, Y. Yuan, X. Zhou, Effect of Excess Li Content on the Microwave Dielectric Properties of the M-Phase of Li_2O-Nb_2O_5-TiO_2 Ceramics, J. Electron. Mater., 43 (2014) 3954-3958.

[13] D. Zhou, L.X. Pang, D.W. Wang, I.M. Reaney, $BiVO_4$ based high k microwave dielectric materials: a review, J. Mater. Chem.C, 6 (2018) 9290-9313.

[14] T. Zhang, R. Zuo, J. Zhang, N. Alford, Structure, Microwave Dielectric Properties, and Low-Temperature Sintering of Acceptor/Donor Codoped $Li_2Ti_{1-x}(Al_{0.5}Nb_{0.5})_xO_3$Ceramics, J. Am. Ceram. Soc., 99 (2016) 825-832.

[15] Q. Liao, L. Li, X. Ding, X. Ren, P. Kabos, A New Temperature Stable Microwave Dielectric Material $Mg_{0.5}Zn_{0.5}TiNb_2O_8$, J. Am. Ceram. Soc., 95 (2012) 1501-1503.

[16] Y. Chen, E. Li, S. Duan, S. Zhang, Low Temperature Sintering Kinetics and Microwave Dielectric Properties of $BaTi_5O_{11}$ Ceramic, ACS Sustain Chem Eng, 5 (2017) 10606-10613.

[17] G. Chen, M. Hou, Y. Bao, C. Yuan, C. Zhou, H. Xu, Silver Co-Firable $Li_2ZnTi_3O_8$ Microwave Dielectric Ceramics with LZB Glass Additive and TiO_2 Dopant, Int. J. Appl. Ceram. Technol., 10 (2013) 492-501.

[18] D. Thomas, P. Abhilash, M.T. Sebastian, Casting and characterization of $LiMgPO_4$ glass free LTCC tape for microwave applications, J. Eur. Ceram. Soc., 33 (2013) 87-93.

[19] S. Duan, E. Li, Y. Chen, B. Tang, Y. Yuan, S. Zhang, Low temperature sintering kinetics of BaO-0.15ZnO-4TiO_2 dielectric ceramic in the presence of a liquid phase, Ceram. Int., 43 (2017) 197-200.

[20] A.Y. Borisevich, P.K. Davies, Effect of V2O5 Doping on the Sintering and Dielectric Properties of M-Phase $Li_{1+x-y}Nb_{1-x-3y}Ti_{x+4y}O_3$ Ceramics, J. Am. Ceram. Soc., 87 (2004) 1047-1052.

[21] Q. Zeng, W. Li, J. l. Shi, J. k. Guo, M. w. Zuo, W. j. Wu, A New Microwave Dielectric Ceramic for LTCC Applications, J. Am. Ceram. Soc., 89 (2006) 1733-1735.

[22] P. Zhang, L. Li, G. Li, W. Zhang, Low temperature sintering of $Li_{1.1}Nb_{0.58}Ti_{0.5}O_3$-x$Bi_2O_3$ dielectric with adjustable temperature coefficient, J. Mater. Sci. Mater. Electron., 21 (2009) 213-217.

[23] T. Tabaru, K. Shobu, H. Hirai, S. Hanada, Influences of Al content and secondary phase of $Mo_5(Si,Al)_3$ on the oxidation resistance of Al-rich $Mo(Si,Al)_2$-base composites, Intermetallics, 11 (2003) 721-733.

[24] D. Hotza, P. Greil, Aqueous Tape Casting of Ceramic Powders, Mater. Sci. Eng., A, 202 (1995) 206-217.

[25] E. Li, N. Niu, J. Wang, S. Yu, S. Duan, Y. Yuan, Effect of Li–B–Si glass on the low temperature sintering behaviors and microwave dielectric properties of the Li-modified ss-phase Li_2O–Nb_2O_5–TiO_2 ceramics, J. Mater. Sci. - Mater. Electron., 26 (2015) 3330-3335.

[26] H. Yang, E. Li, H. Yang, H. He, R.S. Zhang, Synthesis of $Zn_{0.5}Ti_{0.5}NbO_4$ microwave dielectric ceramics with Li_2O-B_2O_3-SiO_2 glass for LTCC application, Int. J. Appl. Glass Sci., 9 (2018) 392-402.

[27] E. Li, H. Yang, H. Yang, S. Zhang, Effects of Li_2O-B_2O_3-SiO_2 glass on the low-temperature sintering of $Zn_{0.15}Nb_{0.3}Ti_{0.55}O_2$ ceramics, Ceram. Int., 44 (2018) 8072-8080.

[28] M.M. Mao, X.M. Chen, X.Q. Liu, Structure and Microwave Dielectric Properties of Solid Solution in $SrLaAlO_4$-Sr_2TiO_4 System, J. Am. Ceram. Soc., 94 (2011) 3948-3952.

[29] R.D. Shannon, Dielectric polarizabilities of ions in oxides and fluorides, J. Appl. Phys., 73 (1993) 348-366.

[30] D. Zhou, L. X. Pang, J. Guo, Y. Wu, G. Q. Zhang, W. Dai, H. Wang, X. Yao, J.B. Lim, New Microwave Dielectric Ceramics $BaLn_2(MoO_4)_4$ (Ln = Nd and Sm) with Low Loss, J. Am. Ceram. Soc., 94 (2011) 2800-2803.

[31] Y. Wang, R. Zuo, C. Zhang, J. Zhang, T. Zhang, N. Alford, Low-Temperature-Fired $ReVO_4$(Re = La, Ce) Microwave Dielectric Ceramics, J. Am. Ceram. Soc., 98 (2015) 1-4.

[32] D. Zhou, C.A. Randall, L.X. Pang, H. Wang, J. Guo, G.Q. Zhang, Y. Wu, K.T. Guo, L. Shui, X. Yao, Microwave dielectric properties of $(ABi)_{1/2}MoO_4$ (A=Li, Na, K, Rb, Ag) type ceramics with ultra-low firing temperatures, Mater. Chem. Phys., 129 (2011) 688-692.

[33] D. Guo, D. Zhou, W.B. Li, L.X. Pang, Y.Z. Dai, Z.M. Qi, Phase Evolution, Crystal Structure, and Microwave Dielectric Properties of Water-Insoluble (1-x)$LaNbO_4$-x$LaVO_4$ ($0 \leq x \leq 0.9$) Ceramics, Inorg Chem, 56 (2017) 9321-9329.

[34] C. Zhang, R. Zuo, J. Zhang, Y. Wang, J. Jones, Structure-Dependent Microwave Dielectric Properties and Middle-Temperature Sintering of Forsterite $(Mg_{1-x}Ni_x)_2SiO_4$Ceramics, J. Am. Ceram. Soc., 98 (2015) 702-710.

[35] D. Zhou, H. Wang, X. Yao, Microwave dielectric properties and co-firing of $BiNbO_4$ ceramics with CuO substitution, Mater. Chem. Phys., 104 (2007) 397-402.

[36] A.J. Bosman, E.E. Havinga, Temperature Dependence of Dielectric Constants of Cubic Ionic Compounds, Phys Rev, 129 (1963) 1593-1600.

[37] H. Lee, K.S. Hong, S. Kim, I. Kim, DIELECTRIC PROPERTIES OF MNb_2O_6 COMPOUNDS (WHERE M = Ca, Mn, Co, Ni, OR Zn), Mater. Res. Bull., 32 (1997) 847-855.

[38] S.H. Yoon, D.W. Kim, S.Y. Cho, K.S. Hong, Investigation of the relations between structure and microwave dielectric properties of divalent metal tungstate compounds, J. Eur. Ceram. Soc., 26 (2006) 2051-2054.

[39] D. Zhou, L.X. Pang, J. Guo, Z.M. Qi, T. Shao, X. Yao, C.A. Randall, Phase evolution, phase transition, and microwave dielectric properties of scheelite structured $xBi(Fe_{1/3}Mo_{2/3})O_4–(1−x)BiVO_4$ $(0.0 \leq x \leq 1.0)$ low temperature firing ceramics, J. Mater. Chem., 22 (2012) 21412.

[40] E. Li, Y. Chen, J. Xiong, M. Zou, B. Tang, Low-temperature firing and microwave dielectric properties of Ba–Nd–Ti with composite doping Li–B–Si and Ba–Zn–B glasses, J. Mater. Sci. - Mater. Electron., 27 (2016) 8428-8432.

[41] L.X. Pang, H. Wang, D. Zhou, X. Yao, Low-temperature sintering and microwave dielectric properties of TiO_2-based LTCC materials, J. Mater. Sci. Mater. Electron., 21 (2010) 1285-1292.

[42] D. Zhou, D. Guo, W.B. Li, L.X. Pang, X. Yao, D.W. Wang, I.M. Reaney, Novel temperature stable high-ε_r microwave dielectrics in the $Bi_2O_3–TiO_2–V_2O_5$ system, J. Mater. Chem.C, 4 (2016) 5357-5362.

[43] Y. Chen, E. Li, M. Zou, H. He, S. Zhang, A synergistic effect of $La_2O_3–B_2O_3–ZnO$ and $V_2O_5–CuO$ glass on the low-temperature sintering of $Ca_{0.6}La_{0.268}TiO_3$ dielectric ceramic, J. Mater. Sci. - Mater. Electron., 28 (2017) 13132-13138.

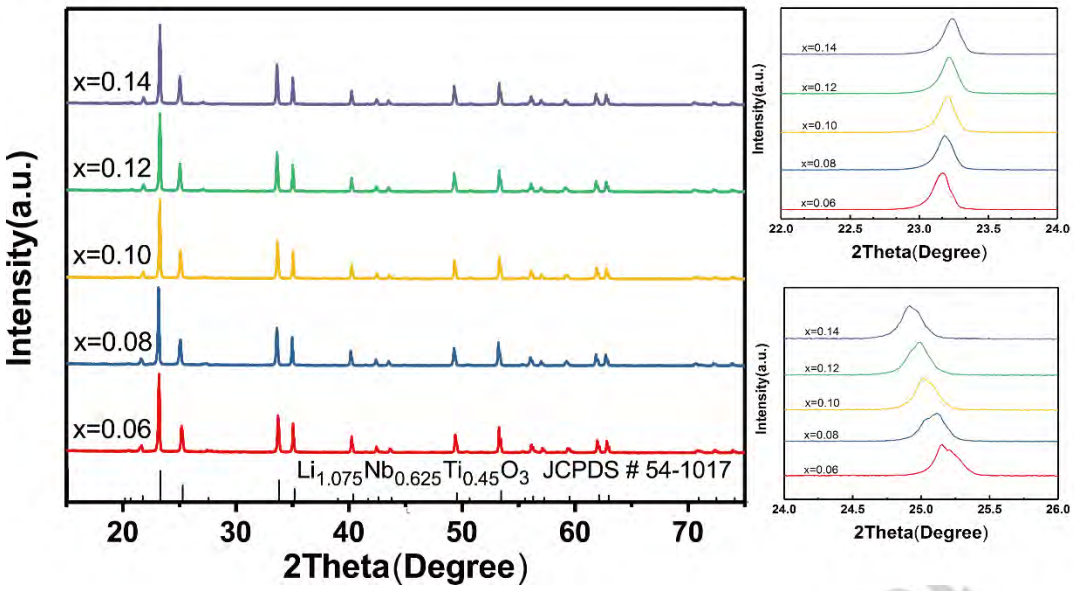

Figure 1. The XRD patterns of LNT ceramics sintered at 1100℃ for 2 h

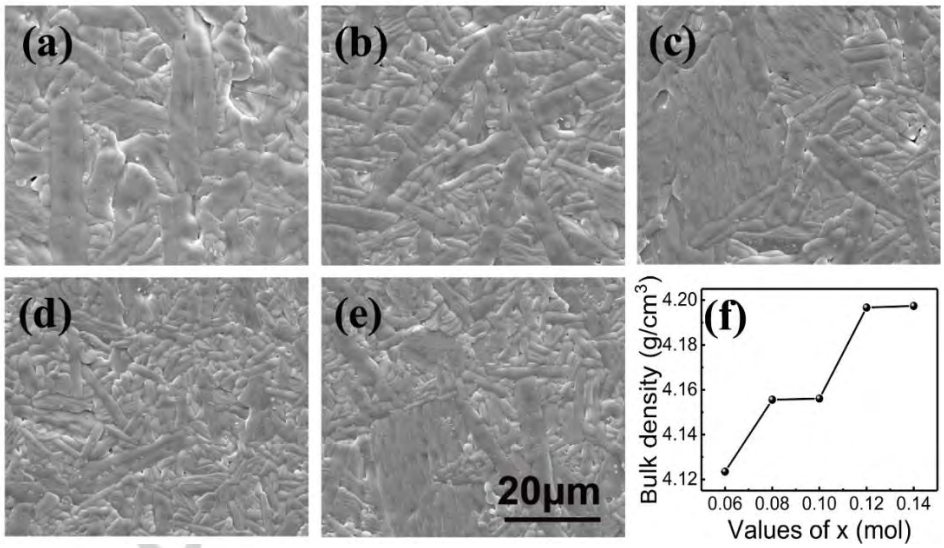

Figure 2. The SEM photograph of LNT ceramics with: (a) x = 0.06, (b) x = 0.08, (c) x = 0.10, (d) x = 0.12, (e) x = 0.14 when sintered at 1100℃ for 2 h and (f) bulk density of ceramics

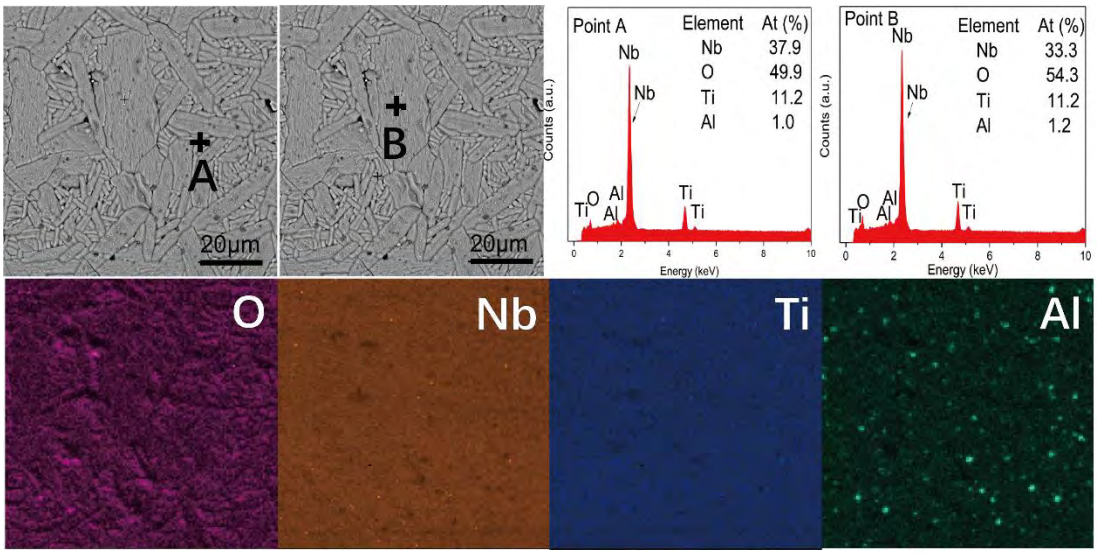

Figure 3. The EDS analysis of spot A and B of LNT ceramic (x = 0.10) and Element mapping of the LNT ceramic (x = 0.10)

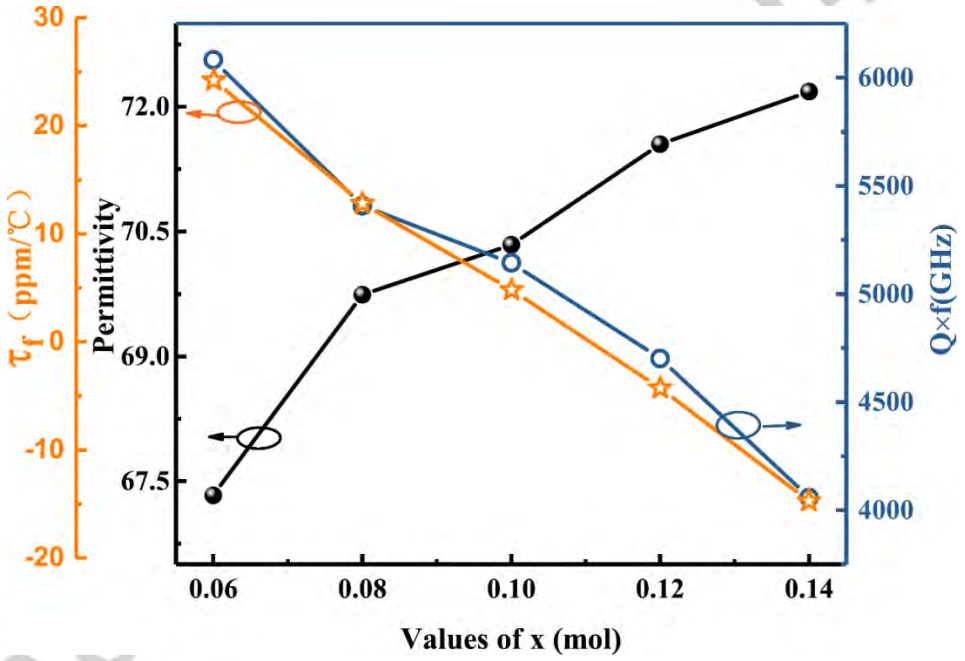

Figure 4. The microwave dielectric properties of LNT ceramic

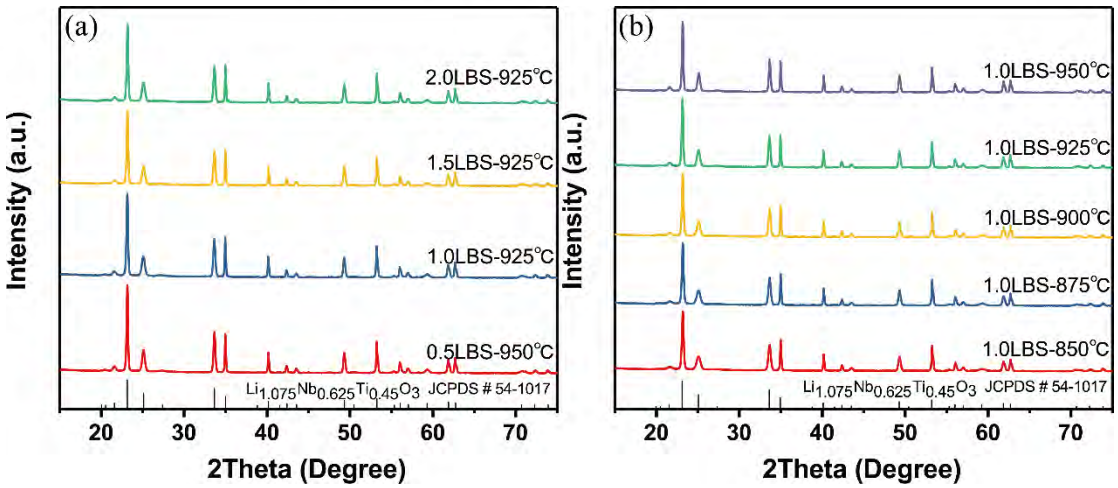

Figure 5. (a) The XRD patterns of the ceramics at optimum sintering temperature for 2 h with different content of LBS glass; (b) The XRD patterns of the ceramics sintered at 850~950 °C with 1.0 wt. % LBS glass.

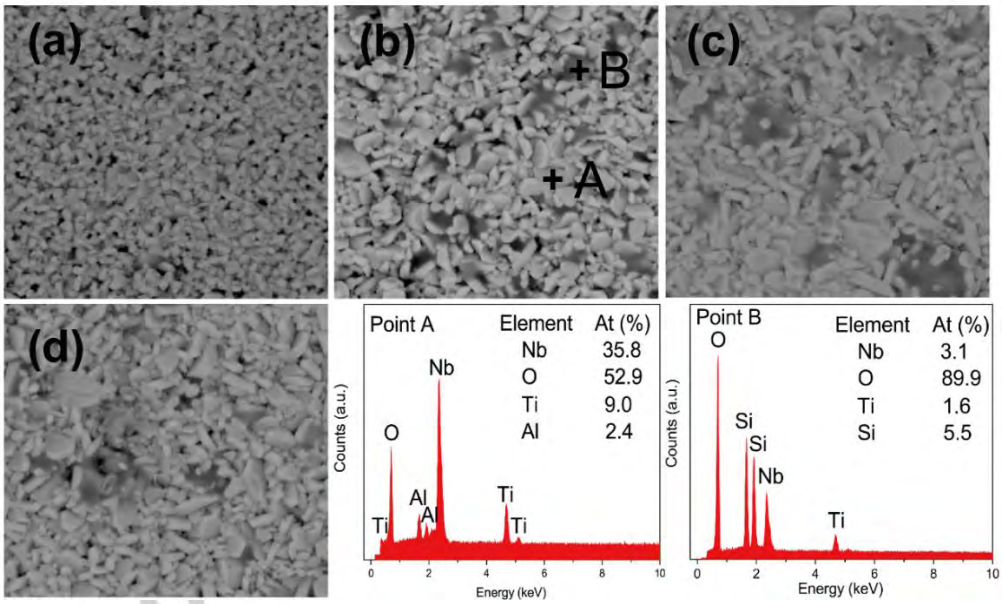

Figure 6. The SEM images of LNT ceramic with different amount of LBS glass sintered at 925℃ (a) 0.5 wt. %, (b) 1.0 wt. %, (c) 1.5 wt. %, (d) 2.0 wt. % and EDS analysis of LNT ceramic (with 1.0 wt. % LBS)

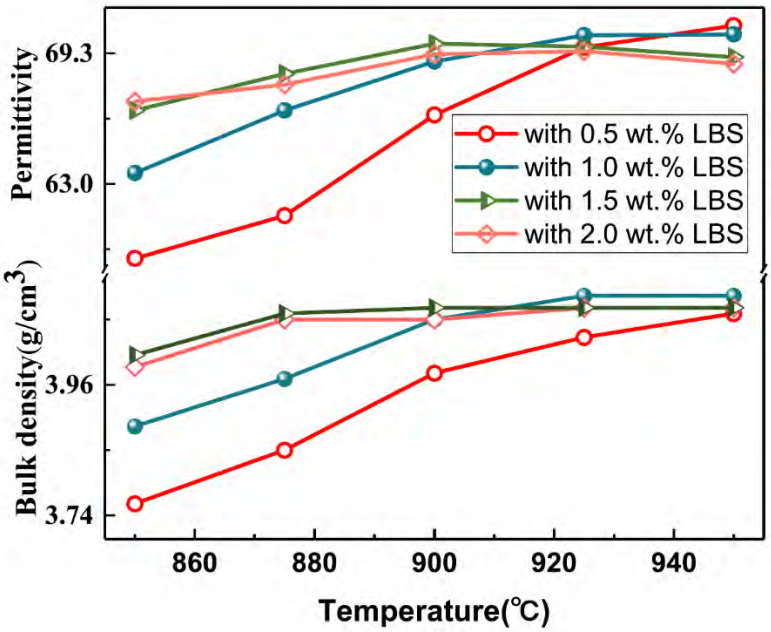

Figure 7. The ε_r value and bulk density of the LNT ceramics with different LBS addition versus sintering temperature

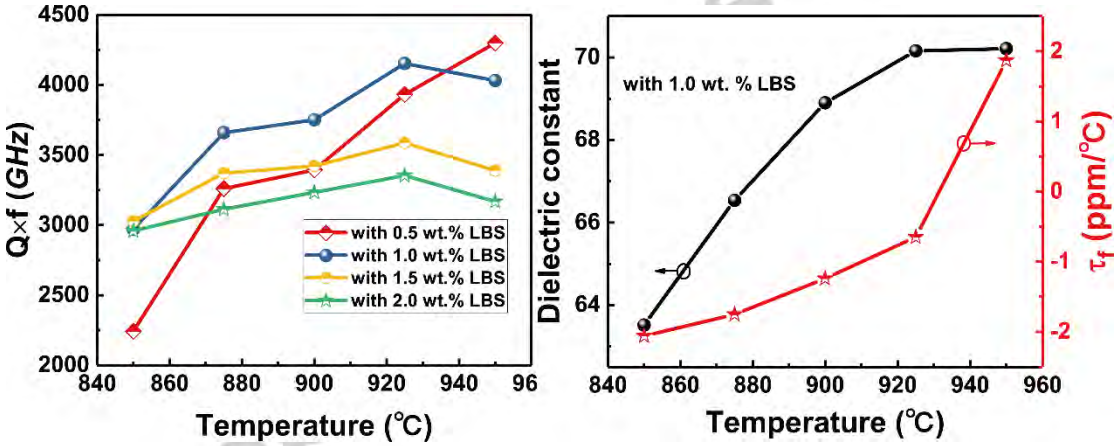

Figure 8. The microwave dielectric properties of the LNT ceramics with different LBS addition versus sintering temperature

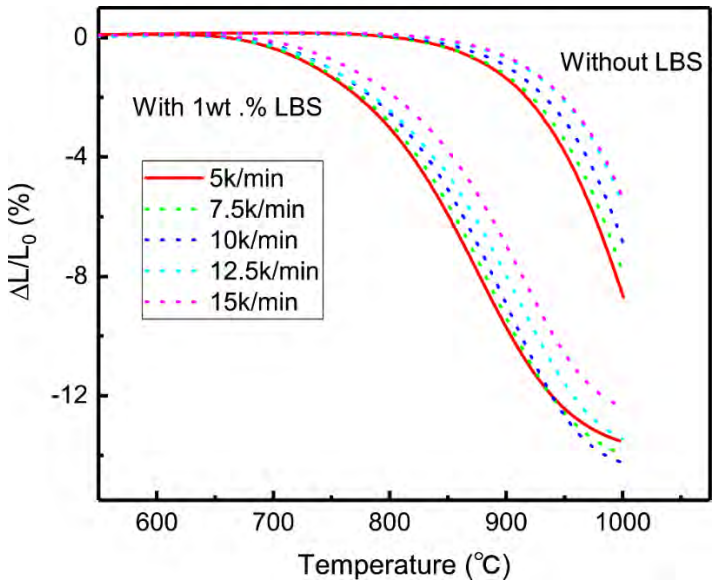

Figure .9 The shrinkage curve of LNT samples undoped and doped with 1.0 wt. % LBS addition.

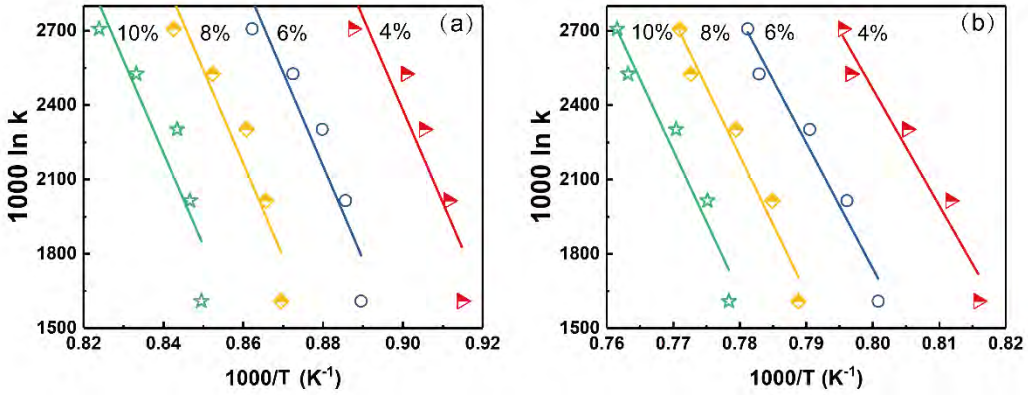

Figure 10. The 1000 ln k as a function of 1/T at different shrinkage, where (a): without LBS, (b) with 1.0 wt. %LBS

Table 1. The lattice parameter of LNT ceramics

x	Cell parameters				V_{unit} (Å^3)
	a=b(Å)	c(Å)	α=β (°)	γ (°)	
0.06	5.11997	13.91466	90	120	315.89
0.08	5.12382	13.90891	90	120	316.24
0.10	5.12567	13.90377	90	120	316.35
0.12	5.12735	13.90351	90	120	316.55
0.14	5.12879	13.90007	90	120	316.65

Table 2. The microwave dielectric properties of typically high ε_r LTCC

Chemical composition	ST (℃)	ε_r	$Q\times f\,(GHz)$	τ_f (ppm/℃)	Ref.
0.02BFM -0.98BV	820	72.9±0.2	13500±300	-270	39
0.10BFM -0.90BV	820	74.8±0.2	11600±300	+170	39
0.02BFM -0.98BV+0.10BFM -0.90BV	820	74.8±0.2	13000±300	+20	39
BNT+3.0 wt.%LBS+3.0 wt.% BZB	900	69.78	4416	46.05	40
$Zn_{0.15}Nb_{0.3}Ti_{0.55}O_2$+1.5 wt.% LBS	900	73.59	8024	270.54	27
$0.08Bi_2Ti_4O_{11}$+2.0 wt.% CuO	900	81	3500	-5.1	41
$0.45BV–0.55TiO_2$	900	86	9500	-8	42
CLT+3.0 wt.% LBZ+1.0 wt.% VC	900	98.94	4885	305.17	43
$Bi_2(Li_{0.5}Ta_{1.5})O_7$+2.0 mol.% Bi_2O_3	920	64.1	11200	-19	3
This Work	925	70.16	4153	-0.65	

BFM: $Bi(Fe_{1/3}Mo_{2/3})O_4$; BV: $BiVO_4$; BNT: $BaNd_2Ti4O_{12}$; CLT:$Ca_{0.6}La_{0.268}TiO_3$